# Static Analysis of Structural Systems with Uncertain Parameters Using Probability-Box

Naijia Xiao[1), Robert Mullen[2) and Rafi Muhanna[1)
[1) *School of Civil and Environmental Engineering, Georgia Institute of Technology, Atlanta, GA 30332, USA, {naijia.xiao, rafi.muhanna}@gatech.edu*
[2) *Department of Civil and Environmental Engineering, University of South Carolina, Columbia, SC 29208, USA, rlm@sc.edu*

**Abstract:** A static analysis of structural systems with uncertain parameters is presented. Uncertain load and material parameters of the system are modeled by probability-boxes (or p-boxes), which do not require complete information about the statistical nature of the underlying random process. Arithmetic operations on p-boxes yield guaranteed lower and upper bounds on the probability distribution of the solution, regardless of the dependency among those uncertain parameters. In this paper, both load and material uncertainties for the first time are handled using a non-Monte-Carlo p-box approach that guarantees to enclose the exact solution. The governing linear equations are solved by an iterative approach that exploits a fixed-point formulation of the system of linear equations. In order to reduce overestimation and obtain the tightest bounds possible, a decomposition of the stiffness matrix of the structure is adopted. The resulting formulation gives guaranteed lower and upper bounds of the probability distribution of the structural responses, at a high computational efficiency and a low overestimation level.

**Keywords:** uncertainty, probability-box, matrix decomposition, iterative enclosure method

## 1. Introduction

Real systems contains uncertainties that cause discrepancy between the performance of the theoretical model and the real system (Fernández-Martínez et al., 2013). Conventional treatment of uncertainties involves probability theory, which models uncertain parameter in the system using random variables (Kolmogorov, 1950). This probabilistic approach successfully handles problems when the statistical nature of the uncertainty is well understood. Thus it is suitable when only allegoric uncertainties are present. However, when the nature of the uncertainty is not well understood and epistemic uncertainties are present (Moens and Hanss, 2011; Zhang, 2005), alternative approaches are proposed, such as Bayesian network (Igusa et al., 2002; Soize, 2013), fuzzy sets (Dehghan et al., 2006; Klir and Wierman, 1999), evidence theory (Dempster, 1967; Shafer, 1968), and intervals (Alefeld and Herzberger, 1984; Kulisch and Miranker, 1981; Moore et al., 2009; Muhanna et al., 2007).

The probability-box approach (or more compactly, p-box) integrates the conventional probability theory with the concept of intervals (Augustin and Hable, 2010; Beer, et al., 2013; Ferson, 2002). A p-box gives the lower and upper bounds on the cumulative distribution function (CDF) for an uncertain variable. It is subject to any legitimate CDF within the given lower and upper bounds. Hence a traditional random variable can be interpreted as a p-box with zero width, and an interval can be interpreted as a rectangular p-box with constant width (Ferson, 2002).

One of the advantage of the p-box approach is the incorporation of bounded dependence information. In application of conventional probability theory, dependence of two random variables are simplified to their covariance or correlation coefficient (Cui and Blockley, 1990; Davis and Hall, 2003; Lucas, 1995). For linear dependence, the correlation coefficient is either 1 (perfect dependence) or −1 (opposite dependence). For independent variables, the correlation coefficient is 0. Then information about the covariance or correlation is used to analyse the random variables under consideration. Complete information about dependence is given by a joint probability distribution. However, it is often measured by limited information as covariance correlation coefficient (Ferson, et al., 2004). For instance, it is easy to construct two random variables that has 0 correlation coefficient but nonlinear dependence. Thus a more vigorous approach is required when available data is scarce and the consequence is high.

The p-box approach is designed to consider unknown dependence between random variables (Ferson, et al., 2004; Williamson, 1989). The p-box approach uses copulas (Kimeldorf and Sampson, 1975; Nelsen, 1999; Sklar, 1959), which gives complete information about the dependence of two random variables. Specifically, lower and upper bounds of the copula is used when performing binary arithmetic operations on p-boxes, such as addition, subtraction, multiplication, and division. In addition, due to the duality theorem (Frank and Schweizer, 1979; Williamson, 1989), the convolution of p-box, which is originally performed on the bounds of the CDF for given value on the random variable, can be performed on the bounds of the random variable for a given probability level. This significantly improves computational efficiency and facilitates discretization. Detailed discussion on p-boxes and their arithmetic operations can be found in Ferson (2002) and Williamson (1989).

In this paper, the p-box approach is applied to solve structural static problems with uncertain parameters. Both uncertainties in load and in material are considered. To reduce overestimation, a decomposition strategy (Muhanna and Mullen, 2001; Xiao, 2015) is presented, and a fixed-point formulation (Xiao, 2015; Xiao, et al., 2015) is implemented to solve the resulting governing linear system. To illustrate the performance of the current method, two numerical examples are solved, and the solutions are compared with those obtained from other available methods such as the interval Monte Carlo method (Zhang, et al., 2012). The results show that the current algorithm yields a tight p-box that encloses the solution, regardless of the dependence of the random variables.

## 2. Preliminaries on P-Boxes

A probability-box (or p-box) is useful to describe random variables whose probability distributions are not fully known. The p-box approach provides a rigorous way to account for uncertainty in our (lack of) knowledge of the random variables under study (Ferson, et al., 2004) by accounting for unknown dependence of the random variables. Arithmetic operations on p-boxes are developed in a way consistent with conventional probability theory (Ferson, 2002; Williamson, 1989). In the following subsections, some background information about p-boxes are introduced.

### 2.1. Description of a p-box

A p-box is defined by its lower and upper bounds on the cumulative distribution function (CDF) $\underline{F_X}(x)$ and $\overline{F_X}(x)$. It represents all legitimate random distributions whose CDF lie within that range. For a given value of $x$, the lower bound $\underline{F_X}(x)$ means the lowest probability that the random variable $X$ is smaller than $x$, and the upper bound $\overline{F_X}(x)$ means the highest probability that $X$ is smaller than $x$ (Williamson, 1989).

The inverse functions of $\underline{F_X}(x)$ and $\overline{F_X}(x)$ gives the respective upper and lower bounds of a range $[\underline{x}, \overline{x}]$ of the random variable $X$ for a given probability level $F_X$. For a given value of $F_X$, $\overline{F_X}^{-1}(F_X)$ is the smallest $x$ such that the probability of $X$ is smaller than $x$ is $F_X$, and $\underline{F_X}^{-1}(F_X)$ is the largest, where superscript $^{-1}$ means inverse function. Note that the lower bound function $\underline{F_X}(x)$ corresponds to the upper bound $\overline{x}$ for a given $F_X$, and *vice versa*.

For a discrete description of a p-box, a list of triples $[m_i, \underline{x}_i, \overline{x}_i]$ are used (Dubois and Prade, 1991; Zhang, et al., 2012), where $m_i$ are the probability masses, and $[\underline{x}_i, \overline{x}_i]$ are the associated intervals. The $i$-th probability mass $m_i$ can be viewed as the probability that the $i$-th focal element $[\underline{x}_i, \overline{x}_i]$ is the range of $x$. For convenience, the probability masses have the same value for all focal elements, i.e., $m_i = 1/m$, where $m$ is the number of focal elements in the discretization.

### 2.2. Dependency and copulas

The complete dependence information between two random variables are described by their joint probability distribution, which can be specified by a joint probability density function or a joint cumulative distribution function (Ferson, et al., 2004; Nelsen, 1999; Sklar, 1959). Because we are primarily dealing with CDF in p-boxes, the latter approach is adopted here.

For given random variables $X$ and $Y$, any joint cumulative distribution function $F_{XY}(X, Y)$ can be expressed in terms of marginal distribution functions $F_X(x)$ and $F_Y(y)$ via the introduction of a 2D mapping $C(a, b) : [0, 1] \times [0, 1] \mapsto [0, 1]$

$$F_{XY}(X, Y) = C\left(F_X(x), F_Y(y)\right). \tag{1}$$

In the above equation, the 2D mapping $C(u, v)$ is a copula, satisfying the following requirements:

- $C(a, 0) = C(0, a) = 0$ and $C(a, 1) = C(1, a) = a$ for all $a \in [0, 1]$;
- $C(a_1, b_1) + C(a_2, b_2) - C(a_1, b_2) - C(a_2, b_1) \geq 0$ for all $a_1, a_2, b_1, b_2 \geq 0$ such that $a_1 \leq a_2$ and $b_1 \leq b_2$.

Any arbitrary copula $C(u, v)$ satisfies

$$W(u, v) \leq C(u, v) \leq M(u, v), \tag{2}$$

where $W(u, v) = \max(u + v - 1, 0)$ and $M(u, v) = \min(u, v)$ are the lower and upper Fréchet-Hoeffding bounds for any copula, respectively (Fréchet, 1951; Hoeffding, 1940). The lower bound $W(u, v)$ represents an opposite dependence between two distributions, and the upper bound $M(u, v)$

represents a perfect dependence. As a side note, independent case is represented by the copula $\Pi(u, v) = uv$. The dual of a copula is defined as

$$C^*(u, v) = u + v - C(u, v). \tag{3}$$

Parametrized copulas can be used to model dependence of different strength. One class of copulas, the Archimedean class, is associative and admits an explicit formula (Nelsen, 1999). The Archimedean copula has the following form

$$C_\theta(u, v) = \psi_\theta^{-1}\left(\psi_\theta(u) + \psi_\theta(v)\right), \tag{4}$$

where $\psi_\theta : [0, 1] \mapsto [0, \infty)$ is the generator function, which is continuous, strictly decreasing, convex, and $\psi_\theta(1) = 0$. Some of the most important families of Archimedean copulas include:

- The Clayton family (Clayton, 1978), with generator function $\psi_\theta(x) = (x^{-\theta} - 1)/\theta$,

$$C_\theta(u, v) = \left(u^{-\theta} + v^{-\theta} - 1\right)^{-1/\theta}, \tag{5}$$

  where $\theta \geq -1$. The perfect dependence corresponds to $\theta = \infty$, the opposite dependence is $\theta = -1$, and the independent case is $\theta = 0$.

- The Frank family (Frank, 1979), with generator function $\psi_\theta(x) = \ln\left(\dfrac{e^{-\theta} - 1}{e^{-x\theta} - 1}\right)$,

$$C_\theta(u, v) = \frac{1}{\theta}\ln\left(1 + \frac{(e^{-u\theta} - 1)(e^{-v\theta} - 1)}{e^{-\theta} - 1}\right), \tag{6}$$

  where $\theta \in \mathbb{R}$. The perfect dependence corresponds to $\theta = -\infty$, the opposite dependence is $\theta = \infty$, and the independent case is $\theta = 0$.

The above discussion is restricted to bivariate case for two random variables $X$ and $Y$, but the idea can be easily extended to multi-variate case as well.

### 2.3. Arithmetic operations on p-boxes

For a single p-box $X$, its negation, its reciprocal, and its multiplication with a real number are all p-boxes. For instance, consider its negation $Y = -X$. Assume the lower and upper bound functions are $\underline{F_X}(x)$ and $\overline{F_X}(x)$, respectively. Then

$$\underline{F_Y}(y) = 1 - \overline{F_X}(-y), \qquad \overline{F_Y}(y) = 1 - \underline{F_X}(-y). \tag{7}$$

If the discrete description is used, and the focal elements are $[\underline{x}_i, \overline{x}_i]$, the results are

$$[\underline{y}_i, \overline{y}_i] = [-\overline{x}_{m+1-i}, -\underline{x}_{m+1-i}], \tag{8}$$

where $m$ is the number of focal elements.

For two p-boxes $X$ and $Y$, the result of their arithmetic binary operations, such as addition, subtraction, multiplication, and division, is also a p-box. The result depends on the lower and upper bounds of their respective CDF's, as well as the copula between $X$ and $Y$. According to Williamson (1989), for two p-boxes $X$ and $Y$, the lower and upper bounds of the CDF of the sum $Z = X + Y$ are given by

$$\underline{F_Z}(z) = \sup_{v \in \mathbb{R}} C\big(\underline{F_X}(z-v),\, \underline{F_Y}(v)\big), \qquad \overline{F_Z}(z) = \inf_{v \in \mathbb{R}} C^*\big(\overline{F_X}(z-v),\, \overline{F_Y}(v)\big), \tag{9}$$

where $C(u, v)$ is the known lower bound of the copula between $X$ and $Y$, and $C^*(u, v)$ is its dual. For discrete description, the $i$-th focal element of the sum, i.e., $[\underline{z}_i, \overline{z}_i]$, is given by

$$\underline{z}_i = \sup_{j,\, k \in C_i^*} (\underline{x}_j + \underline{y}_k), \qquad \overline{z}_i = \inf_{j,\, k \in C_i} (\overline{x}_j + \overline{y}_k), \tag{10}$$

where $j,\, k \in C_i$ means that $j$ and $k$ satisfy $\frac{i-1}{m} \in C([\frac{j-1}{m},\, \frac{j}{m}],\, [\frac{k-1}{m},\, \frac{k}{m}])$, and $j,\, k \in C_i^*$ means that $j$ and $k$ satisfy $\frac{i}{m} \in C^*([\frac{j-1}{m},\, \frac{j}{m}],\, [\frac{k-1}{m},\, \frac{k}{m}])$. For the Fréchet-Hoeffding lower bound copula $W(u, v) = \max(u + v - 1, 0)$, Eq. (10) becomes

$$\underline{z}_i = \sup_{j \in [1,\, i]} (\underline{x}_j + \underline{y}_{i+1-j}), \qquad \overline{z}_i = \inf_{j \in [i,\, m]} (\overline{x}_j + \overline{y}_{i+m-j}) \tag{11}$$

For multiple p-boxes $X_i$, when the dependence coefficient $\theta$ is constant, both the addition and the multiplication are associative. The results do not depend on the order of the arithmetic operations performed. Operations on vector and matrix with p-box entries can be defined accordingly. However, for each binary arithmetic operation ($+,\ -,\ \times,$ or $\div$), the corresponding dependence coefficient $\theta$ or the copula $C_\theta(u, v)$ in general must be specified. In practice, this is not always possible. Hence the usual practice is to specify $\theta$ corresponding to the lower and upper bounds of the copulas. For positive dependence, the lower bound $\underline{\theta} = 0$ and the upper bound $\overline{\theta} = \infty$ for both the Clayton family and the Frank family. For negative dependence, $\underline{\theta} = -\infty$ and $\overline{\theta} = 0$ for the Clayton family, and $\underline{\theta} = -1$ and $\overline{\theta} = 0$ the Frank family. In both cases, the independent case is included as a subset. Hence the yielded solution considers the least favorable circumstances possible and encloses the solutions assuming independence, as observed in the comparison with the interval Monte Carlo solution (Zhang, et al., 2012) in the numerical example section.

For a more comprehensive discussion on arithmetic operations of p-boxes, we refer to the work of Ferson (2002) and Williamson (1989). In particular, Ferson (2002) considers binary arithmetic operations under the independence assumption.

## 3. Finite Element Formulation

Many engineering problems can be reduced to solving the following linear system of equations. For instance, for structural static analysis, after a displacement-based Finite Element (FE) discretization (Bathe and Wilson, 1976; Cook, et al., 2007), the system governing equation is

$$\mathbf{K}\mathbf{u} = \mathbf{f}, \tag{12}$$

where $\mathbf{K}$ is the stiffness matrix, $\mathbf{f}$ is the equivalent load vector, and $\mathbf{u}$ is the unknown displacement vector. The goal is to solve for the unknown displacement vector $\mathbf{u}$ when the external load and the structure itself are given. When the system contains uncertain parameters, and those parameters are modeled by p-boxes, matrix $\mathbf{K}$ and vector $\mathbf{f}$ contain p-box entries. As a result, the unknown vector $\mathbf{u}$ also contains p-box entries. The goal of the current section is to develop an algorithm to solve the linear system Eq. (12) when p-box entries are present.

Following our previous work on interval linear systems (Xiao, 2015), to reduce overestimation in the interval of the final solution, the stiffness matrix $\mathbf{K}$ and the equivalent load vector $\mathbf{f}$ are decomposed into a form that minimize the multiple occurrences of the same p-box (Muhanna and Mullen, 2001). In addition, parametrized copulas are introduced to model dependence among uncertain parameters. Finally, the linear system Eq. (12) is solved using an iterative approach (Neumaier and Pownuk, 2007) by transforming the governing equation into a fixed-point form. Detailed discussions are presented in the following subsections.

### 3.1. Matrix decomposition strategy

The following decomposition of the stiffness matrix $\mathbf{K}$ and the equivalent load vector $\mathbf{f}$ is presented

$$\mathbf{K}^P = \mathbf{A}\,\mathrm{diag}\left(\boldsymbol{\Lambda}\boldsymbol{\alpha}^P\right)\mathbf{A}^T, \qquad \mathbf{f}^P = \mathbf{F}\boldsymbol{\delta}^P, \tag{13}$$

where the superscripts $^P$ emphasize that these variables contain p-box entries. After decomposition, all the p-box entries are included in vectors $\boldsymbol{\alpha}^P$ and $\boldsymbol{\delta}^P$. The above decomposition eventually reduce the overestimation of the final solution and helps to obtain a tighter bounds, as illustrated in the numerical simulation section.

In practice, the decompositions in Eq. (13) are performed at the element level before assembly. First the element stiffness matrix $\mathbf{K}_e^P$ and the element nodal equivalent load vector $\mathbf{f}_e^P$ are computed. Their decompositions yield the element matrices $\mathbf{A}_e$, $\boldsymbol{\Lambda}_e$, $\mathbf{F}_e$, $\boldsymbol{\alpha}_e^P$, and $\boldsymbol{\delta}_e^P$. These are further assembled into their global counterparts $\mathbf{A}$, $\boldsymbol{\Lambda}$, $\mathbf{F}$, $\boldsymbol{\alpha}^P$, and $\boldsymbol{\delta}^P$. During the assembly, the element-by-element (EBE) (Rama Rao, et al., 2011) assembly is adopted.

For the standard two-node plane truss elements, assume the Young's modulus $E^P$ are modeled as p-boxes. The corresponding element stiffness matrix $\mathbf{K}_e^P$ is given by

$$\mathbf{K}_e^P = \begin{Bmatrix} E^PA/L & 0 & -E^PA/L & 0 \\ 0 & 0 & 0 & 0 \\ -E^PA/L & 0 & E^PA/L & 0 \\ 0 & 0 & 0 & 0 \end{Bmatrix}. \tag{14}$$

where $L$ is the element length. Then $\boldsymbol{\alpha}_e^P$ contains the only p-box $E^P$ in the element, and the corresponding $\mathbf{A}_e$ and $\boldsymbol{\Lambda}_e$ are given by

$$\mathbf{A}_e = \left\{-1 \;\; 0 \;\; 1 \;\; 0\right\}^T, \qquad \boldsymbol{\Lambda}_e = \left\{A/L\right\}, \qquad \boldsymbol{\alpha}_e^P = \left\{E^P\right\}. \tag{15}$$

The element nodal equivalent load vector $\mathbf{f}_e^P$ is decomposed into the form $\mathbf{f}_e^P = \mathbf{F}_e\boldsymbol{\delta}_e^P$ using the $M$-$\boldsymbol{\delta}$ method (Muhanna and Mullen, 2001). Thus the p-box terms in the element load uncertainty vector $\boldsymbol{\delta}_e^P$ is completely separated from the deterministic part $\mathbf{F}_e$ of the equivalent load.

In the element-by-element assembly, the structure is modeled by separated elements and common nodes that connect the elements. As a result, the structural nodal displacement vector $\mathbf{u}^P$ is a collection of all the element nodal displacement vectors $\mathbf{u}_e^P$, and the nodal displacement vector $\mathbf{u}_n^P$ of the common nodes. Then the global stiffness matrix $\mathbf{K}^P$ and nodal equivalent load $\mathbf{f}^P$are assembled from their element counterparts

$$\mathbf{u}^P = \begin{Bmatrix} \mathbf{u}_e^P \\ \vdots \\ \mathbf{u}_e^P \\ \mathbf{u}_n^P \end{Bmatrix}, \qquad \mathbf{K}^P = \begin{Bmatrix} \mathbf{K}_e^P & & \\ & \ddots & \\ & & \mathbf{K}_e^P \\ & & & 0 \end{Bmatrix}, \qquad \mathbf{f}^P = \begin{Bmatrix} \mathbf{f}_e^P \\ \vdots \\ \mathbf{f}_e^P \\ \mathbf{f}_n^P \end{Bmatrix}, \tag{16}$$

where $\mathbf{f}_n^P$ denotes concentrated forces applied directly on the common nodes. The assembly of $\mathbf{A}$, $\mathbf{\Lambda}$, $\mathbf{F}$, $\boldsymbol{\alpha}^P$, and $\boldsymbol{\delta}^P$ is similar. Note that $\mathbf{K}^P$ is a singular matrix.

To eliminate singularity in $\mathbf{K}^P$, the compatibility requirements and boundary conditions are collected into the form of a constraint equation $\mathbf{C}\mathbf{u}^P = \mathbf{0}$ , which is enforced by the introduction of a Lagrangian multiplier $\boldsymbol{\lambda}^P$ into the energy functional $\mathbf{\Pi}^P$ of the system. The resulting governing equation of the system becomes

$$\begin{Bmatrix} \mathbf{K}^P & \mathbf{C}^T \\ \mathbf{C} & \mathbf{0} \end{Bmatrix} \begin{Bmatrix} \mathbf{u}^P \\ \boldsymbol{\lambda}^P \end{Bmatrix} = \begin{Bmatrix} \mathbf{f}^P \\ \mathbf{0} \end{Bmatrix}. \tag{17}$$

Noting the decomposition of $\mathbf{K}^P$ and $\mathbf{f}^P$, the above equation becomes

$$\left( \begin{Bmatrix} \mathbf{A} \\ \mathbf{0} \end{Bmatrix} \mathrm{diag}(\mathbf{\Lambda}\Delta\boldsymbol{\alpha}^P) \begin{Bmatrix} \mathbf{A}^T & \mathbf{0} \end{Bmatrix} + \begin{Bmatrix} \mathbf{K}_0 & \mathbf{C}^T \\ \mathbf{C} & \mathbf{0} \end{Bmatrix} \right) \begin{Bmatrix} \mathbf{u}^P \\ \boldsymbol{\lambda}^P \end{Bmatrix} = \begin{Bmatrix} \mathbf{F} \\ \mathbf{0} \end{Bmatrix} \boldsymbol{\delta}^P, \tag{18}$$

where $\Delta\boldsymbol{\alpha}^P = \boldsymbol{\alpha}^P - \boldsymbol{\alpha}_0$, and $\mathbf{K}_0 = \mathbf{A}\mathrm{diag}(\mathbf{\Lambda}\boldsymbol{\alpha}_0)\mathbf{A}^T$. Preferably, $\boldsymbol{\alpha}_0$ is chosen as the midpoint of the mean of $\boldsymbol{\alpha}^P$. The Lagrangian multiplier $\boldsymbol{\lambda}^P$ denotes negative internal forces between element nodes and common nodes, when the constraint is a compatibility condition; $\boldsymbol{\lambda}^P$ denotes reactions at the supports, when the constraint is an essential boundary condition (Cook, et al., 2007).

### 3.2. Iterative enclosure approach

The decomposed governing Eq. (18) can be brought into the following compact form

$$\mathbf{K}_{g0}\mathbf{u}_g^P = \mathbf{F}_g\boldsymbol{\delta}^P - \mathbf{A}_g\,\mathrm{diag}\left(\mathbf{\Lambda}\Delta\boldsymbol{\alpha}^P\right)\mathbf{A}_g^T\mathbf{u}_g^P. \tag{19}$$

By defining $\mathbf{G} = \mathbf{K}_{g0}^{-1}$, the above equation is rewritten into the following fixed-point form

$$\mathbf{u}_g^P = (\mathbf{G}\mathbf{F}_g)\boldsymbol{\delta}^P - (\mathbf{G}\mathbf{A}_g)\left(\mathbf{A}_g^T\mathbf{u}_g^P \circ \mathbf{\Lambda}\Delta\boldsymbol{\alpha}^P\right), \tag{20}$$

where the following equality has been used

$$\mathrm{diag}\left(\mathbf{\Lambda}\Delta\boldsymbol{\alpha}^P\right)\mathbf{A}_g^T\mathbf{u}_g^P = \mathrm{diag}\left(\mathbf{A}_g^T\mathbf{u}_g^P\right)\mathbf{\Lambda}\Delta\boldsymbol{\alpha}^P = \mathbf{A}_g^T\mathbf{u}_g^P \circ \mathbf{\Lambda}\Delta\boldsymbol{\alpha}^P, \tag{21}$$

where $\circ$ means the element-by-element product of two vectors. The auxiliary variable $\mathbf{v}^P = \mathbf{A}_g^T\mathbf{u}_g^P$, the following fixed-point form is more suitable for developing an iterative scheme

$$\mathbf{v}^P = (\mathbf{A}_g^T\mathbf{G}\mathbf{F}_g)\boldsymbol{\delta}^P - (\mathbf{A}_g^T\mathbf{G}\mathbf{A}_g)\left(\mathbf{v}^P \circ \mathbf{\Lambda}\Delta\boldsymbol{\alpha}^P\right). \tag{22}$$

To obtain a guaranteed enclosure of $\mathbf{v}^P$, we start from the initial guess $\mathbf{v}_0^P = (\mathbf{A}_g^T\mathbf{GF}_g)\boldsymbol{\delta}^P$, and proceed using the following approach

$$\mathbf{v}_{i+1}^P = (\mathbf{A}_g^T\mathbf{GF}_g)\boldsymbol{\delta}^P - (\mathbf{A}_g^T\mathbf{GA}_g)\left(\mathbf{v}_i^P \circ \boldsymbol{\Lambda}\Delta\boldsymbol{\alpha}^P\right). \tag{23}$$

The iteration stops when $\mathbf{v}_i^P$ stops improving. Final solution $\mathbf{u}_{gn}^P$ is obtained by substituting $\mathbf{A}_g^T\mathbf{u}_g^P$ in Eq. (20) with the converged $\mathbf{v}_n^P$.

In the calculation, to reduce the overestimation, the deterministic matrices $(\mathbf{GF}_g)$ and $(\mathbf{GA}_g)$ in Eq. (20) and $(\mathbf{A}_g^T\mathbf{GF}_g)$ and $(\mathbf{A}_g^T\mathbf{GA}_g)$ in Eq. (23) are prepared before the iteration starts. The initial guess $\mathbf{v}_0^P$ is obtained by multiplying the deterministic matrix $(\mathbf{A}_g^T\mathbf{GF}_g)$ with the p-box vector $\boldsymbol{\delta}^P$. During each iteration, firstly $\boldsymbol{\Lambda}\Delta\boldsymbol{\alpha}^P$ is obtained by multiplying the deterministic matrix $\boldsymbol{\Lambda}$ with the p-box vector $\Delta\boldsymbol{\alpha}^P$; secondly $\boldsymbol{\Lambda}\Delta\boldsymbol{\alpha}^P$ is multiplied element-by-element with the p-box vector $\mathbf{v}_i^P$ to yield $\left(\mathbf{v}_i^P \circ \boldsymbol{\Lambda}\Delta\boldsymbol{\alpha}^P\right)$; thirdly $\left(\mathbf{v}_i^P \circ \boldsymbol{\Lambda}\Delta\boldsymbol{\alpha}^P\right)$ is multiplied with the deterministic matrix $(\mathbf{A}_g^T\mathbf{GA}_g)$, which is further subtracted to the initial guess $(\mathbf{A}_g^T\mathbf{GF}_g)\boldsymbol{\delta}^P$. For each arithmetic operations $(+,\ -,\ \times,\ \text{or}\ \div)$ in the calculation, if the two operands are known to be positively dependent, $\theta = 0$ for both the Clayton family and the Frank family; if they are know to be negative dependent, $\theta = -\infty$ for the Clayton family and $\theta = -1$ for the Frank family.

### 3.3. Random field modeling

In the above discussion, the p-box vector $\boldsymbol{\alpha}^P$ contains Young's modulus for each element, and the p-box vector $\boldsymbol{\delta}^P$ contains all the concentrated forces and distributed forces for each element. Usually these variables cannot vary independently, and it is necessary to describe this dependence among entries in $\boldsymbol{\alpha}^P$, $\boldsymbol{\delta}^P$, and other variables such as the displacement vector $\mathbf{u}^P$, the Lagrangian multiplier $\boldsymbol{\lambda}^P$, and the auxiliary variable $\mathbf{v}^P$.

In conventional probability theory, such dependence is described by the covariance or correlation of random variables. Then covariance decomposition technique (or kernel decomposition) such as the Karhumen-Loève expansion (Ghanem and Spanos, 1991; Zhang and Ellingwood, 1994) is applied to the auto-covariance function (or auto-covariance matrix in the discrete case). The goal is to either reduce the number of independent variables required to model the entire random field, or increase the computational efficiency of the algorithm. However, as pointed out by Ferson, et al. (2004), this is usually an over-simplification of the dependence of random variables in reality. The covariance or correlation between two random variables is insufficient to describe the dependence. Instead, a joint probability distribution in the form of either a joint distribution density function or a copula is required to completely describe it.

In this paper, the Clayton family of copulas $C_\theta(u, v)$ and their duel $C_\theta^*(u, v)$ are used to model dependence between random field variables such as Young's modulus (entries in $\boldsymbol{\alpha}^P$) and distributed load (entries in $\boldsymbol{\delta}^P$), as well as other variables such as $\boldsymbol{\alpha}^P$, $\boldsymbol{\delta}^P$, $\mathbf{u}^P$, $\boldsymbol{\lambda}^P$, and $\mathbf{v}^P$. The yielded solution provides guaranteed lower and upper bounds on the CDF's of the quantities of interest. In the following numerical simulation section, a discussion on the performance of the proposed hierarchical structure of the dependence modeling is presented.

## 4. Numerical Examples

The algorithm discussed previously is implemented in the MATLAB environment. Two structural problems are solved to illustrate the performance of the presented method: *i*) a fixed-end bar subject to axial deformation and *ii*) a simply supported symmetric 15-bar truss. The current method is compared with *i*) an interval Monte Carlo method (see Zhang, et al. (2012) for more detail) and *ii*) an analytical solution (only available for the first example). The results show that the current method is able to yield a conservative enclosure of the solution p-box with little overestimation, considering any dependence among the uncertain variables.

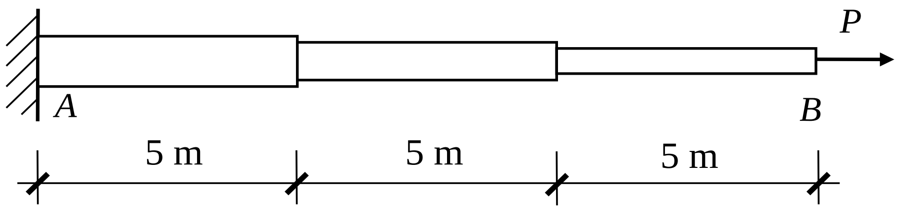


*Figure 1.* A fixed-end bar subject to axial load at the free end.

### 4.1. A fixed-end bar

The first example is a fixed-end bar subject to concentrated load $P$ at the free end, as shown in Figure 1. The p-box for $P$ is bounded from a normal distribution with an interval mean value $\mu_P = [99, 101]$ kN and a standard deviation $\sigma_P = 2$ kN. The total length of the bar is 15 m, which can be divided into three segments of equal length (i.e., $L = 5$ m for each). For each segment, the cross section areas are $A_1 = 0.015$ m$^2$, $A_2 = 0.012$ m$^2$, and $A_3 = 0.010$ m$^2$, respectively. The bar is made of copper, and Young's moduli $E_i$ $(i = 1, 2, 3)$ of the bar are modeled as p-boxes bounded by normal distributions. The interval mean value $\mu_E = [109, 111]$ GPa and the standard deviation $\sigma_E = 2$ GPa. The actual interval mean and standard deviation of $P$ and $E_i$ are given in Table I.

Table I. Bounds on the mean and standard deviation of the contained CDF's in the p-boxes. $P$ - concentrated load; $E_i$ - Young's moduli of the bar in Figure 1.

| | Concentrated load, kN | | | Young's moduli, GPa | |
|---|---|---|---|---|---|
| | Mean $\mu_P$ | Standard deviation $\sigma_P$ | | Mean $\mu_E$ | Standard deviation $\sigma_E$ |
| $P$ | [98.86, 101.14] | [1.142, 3.136] | $E_1$ | [108.9, 111.1] | [1.142, 3.136] |
| | | | $E_2$ | [108.9, 111.1] | [1.142, 3.136] |
| | | | $E_3$ | [108.9, 111.1] | [1.142, 3.136] |

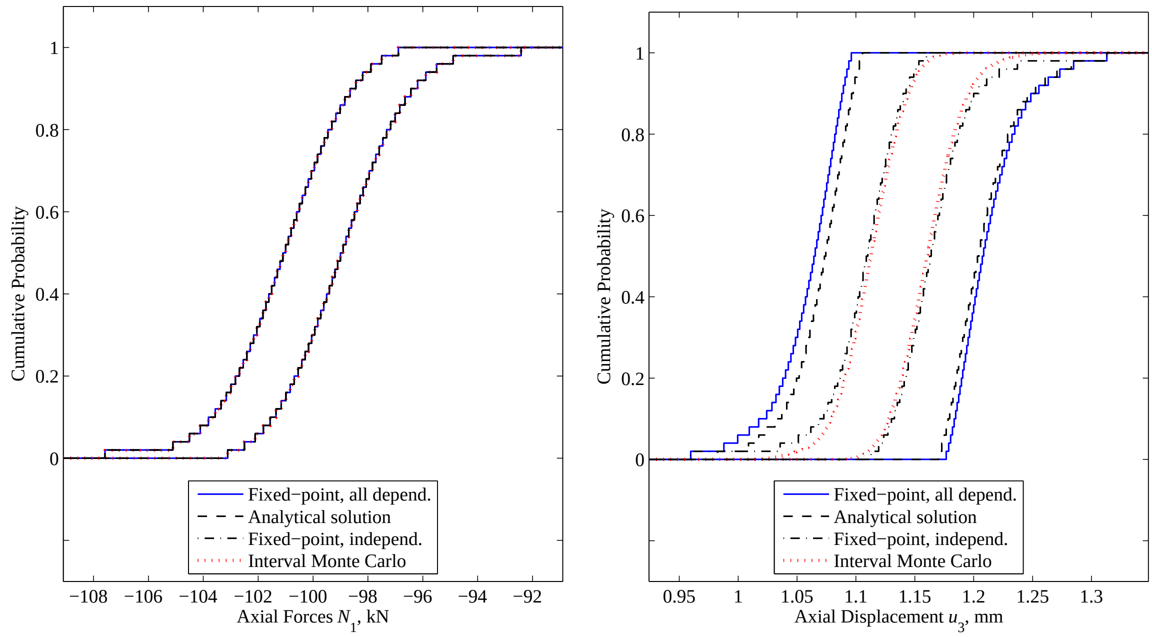


*Figure 2.* P-box solution for the axial force $N_1$ (left half) and axial displacement $u_3$ (right half) of the fixed-end bar of Figure 1, obtained from different method: the current method assuming all dependency (solid lines), the analytical solution (dashed lines), the current method assuming independence (dash-dotted lines), and the interval Monte Carlo method from an ensemble of 100,000 simulations (dotted lines).

A simplified version of the algorithm proposed by Ferson, et al. (2005) is adopted to calculate the interval bounds of mean and standard deviation. In the FEM discretization, the bar is modeled by three truss elements. Since the bar is subject to axial deformation only, lateral displacement is restrained.

The problem has four uncertain parameters, i.e., the concentrated load $P$ and the Young's moduli $E_i$ for each element. Now consider any dependence between the load and the Young's moduli and a positive dependence among $E_i$. The analytic solution to the problem is available. The structure is statically determinate. The axial force in the bar is equal to the concentrated load $P$. The nodal axial displacements

$$u_1 = P\left(\frac{L}{E_1A_1}\right), \quad u_2 = P\left(\frac{L}{E_1A_1} + \frac{L}{E_2A_2}\right), \quad u_3 = P\left(\frac{L}{E_1A_1} + \frac{L}{E_2A_2} + \frac{L}{E_3A_3}\right). \tag{24}$$

Solutions obtained from the current method, the interval Monte Carlo method, and the analytical solution from Eq. (24) are compared with each other. To ensure the accuracy of the solution, 50 focal elements are used in the discretization process. The interval Monte Carlo method include 100,000 simulations, in which the interval solver described in the thesis of Xiao (2015) is used.

All solutions report the same axial force, as shown in the left half of Figure 2. This is not surprising, because the current method can handle load uncertainty without any overestimation

Table II. Bounds on the mean and standard deviation of the contained CDF's in the p-boxes. $N_1$ - axial force; $u_i$ - axial displacements of the bar in Figure 1.

| | Axial force $N_1$, kN | | Axial displacement $u_1$, mm | |
|---|---|---|---|---|
| | Mean $\mu_{N_1}$ | Standard deviation $\sigma_{N_1}$ | Mean $\mu_{u_1}$ | Standard deviation $\sigma_{u_1}$ |
| Current, all depend. | [−101.13, −98.87] | [1.142, 3.136] | [0.2864, 0.3197] | [0.0000, 0.0244] |
| Reference (analytical) | [−101.13, −98.87] | [1.142, 3.136] | [0.2880, 0.3190] | [0.0000, 0.0227] |
| Current, independ. | [−101.13, −98.87] | [1.142, 3.136] | [0.2953, 0.3108] | [0.0030, 0.0172] |
| Interval Monte Carlo | [−101.14, −98.88] | [1.127, 3.096] | [0.2965, 0.3098] | [0.0036, 0.0145] |
| | Axial displacement $u_2$, mm | | Axial displacement $u_3$, mm | |
| | Mean $\mu_{u_2}$ | Standard deviation $\sigma_{u_2}$ | Mean $\mu_{u_3}$ | Standard deviation $\sigma_{u_3}$ |
| Current, all depend. | [0.6381, 0.7255] | [0.0000, 0.0595] | [1.0586, 1.2141] | [0.0000, 0.1033] |
| Reference (analytical) | [0.6436, 0.7232] | [0.0000, 0.0551] | [1.0689, 1.2100] | [0.0000, 0.0954] |
| Current, independ. | [0.6637, 0.6999] | [0.0048, 0.0380] | [1.1055, 1.1673] | [0.0068, 0.0631] |
| Interval Monte Carlo | [0.6672, 0.6970] | [0.0063, 0.0303] | [1.1120, 1.1617] | [0.0094, 0.0482] |

due to the adoption of the $M$-$\boldsymbol{\delta}$ method proposed by Muhanna and Mullen (2001). The right half of Figure 2 compares the axial displacements $u_3$ at the free end from different methods. Note that solution obtained from the current method enclose the analytical solution, with very small overestimation, while the interval Monte Carlo solution is enclosed by the current method a with very large underestimation.

To illustrate that the difference is indeed caused by the inclusion of all dependency of random variables, not by the overestimation in the current method, the solution obtained from the current method assuming independence between random variables is added in Figure 2. Its difference with the interval Monte Carlo solution is very small. Table II compares the interval bounds of the mean and standard deviation of the axial force $N_1$ and axial displacements $u_1$, $u_2$, and $u_3$ obtained from different methods. Some of the lower bounds of the standard deviation obtained from the current method and the analytical solution are zero. This is consistent with the observation that those p-boxes are able to enclose step functions, which correspond to zero standard deviation (the smallest possible bound of the standard deviation of any probability distribution).

Table III. Computational time of the fixed-end bar (Example 4.1) and the simple truss (Example 4.2) for different methods.

| | Fixed-end bar (s) | Simple truss (s) |
|---|---|---|
| Fixed-point, all dependency | 0.41 | 13.20 |
| Fixed-point, independent | 0.07 | 2.27 |
| Interval Monte Carlo | 573.93 | 907.68 |
| Analytical solution | 0.01 | N/A |

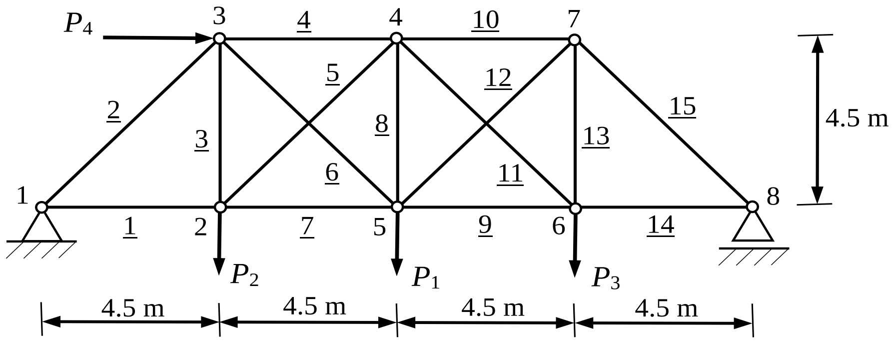


*Figure 3.* An 8-joint 15-bar symmetric simple truss subject to point loads.

Table III lists the computational time of the current example (and the next example) for different methods. The current method is more efficient than the interval Monte Carlo method.

## 4.2. A symmetric simple truss

The second example is a simply supported symmetric truss composed of 15 bars, as shown in Figure 3. The joints are labeled from 1 to 8, and the bars are labeled from $\underline{1}$ to $\underline{15}$. Point loads $P_1$, $P_2$, $P_3$, and $P_4$ are applied at joints 5, 2, 6, and 3, respectively. They are bounded by normal distributions with interval mean values $\mu_{P_1} = [199, 201]$ kN, $\mu_{P_2} = \mu_{P_3} = [99, 101]$ kN, and $\mu_{P_4} = [89, 91]$ kN and standard deviation $\sigma_{P_1} = \sigma_{P_2} = \sigma_{P_3} = \sigma_{P_4} = 2$ kN. Bars $\underline{1}$ to $\underline{3}$, $\underline{13}$ to $\underline{15}$ have the same cross section area $A = 1.0 \times 10^{-3}$ m$^2$, and all other bars, that is, bars $\underline{4}$ to $\underline{12}$, have a smaller cross section area $A = 6.0 \times 10^{-4}$ m$^2$. All the bars are made of steel and their Young's moduli $E_i$ are modeled by p-boxes bounded by normal distributions with an interval mean value $\mu_E = [198, 202]$ GPa and a standard deviation $\sigma_E = 4$ GPa. The corresponding actual mean and standard deviation of $P_i$ and $E_i$ are given in Table IV.

Assume that the concentrated loads can be any dependence, and the Young's moduli of the bars are positively dependent with each other. No further assumptions are made. The axial forces in bar $\underline{2}$ and bar $\underline{8}$ (i.e., $N_2$ and $N_8$) and the displacements at node 5 (i.e., $u_5$ and $v_5$) are solved and

Table IV. Bounds on the mean and standard deviation of the contained CDF's in the p-boxes. $P_i$ - concentrated loads; $E_i$ - Young's moduli of the truss in Figure 3.

| | Concentrated load, kN | | | Young's moduli, GPa | |
|---|---|---|---|---|---|
| | Mean $\mu_P$ | Standard deviation $\sigma_P$ | | Mean $\mu_E$ | Standard deviation $\sigma_E$ |
| $P_1$ | [198.87, 201.13] | [1.142, 3.136] | $E_i$ | [197.7, 202.3] | [2.285, 6.271] |
| $P_2$ | [98.87, 101.13] | [1.142, 3.136] | | | |
| $P_3$ | [98.87, 101.13] | [1.142, 3.136] | | | |
| $P_4$ | [88.87, 91.13] | [1.142, 3.136] | | | |

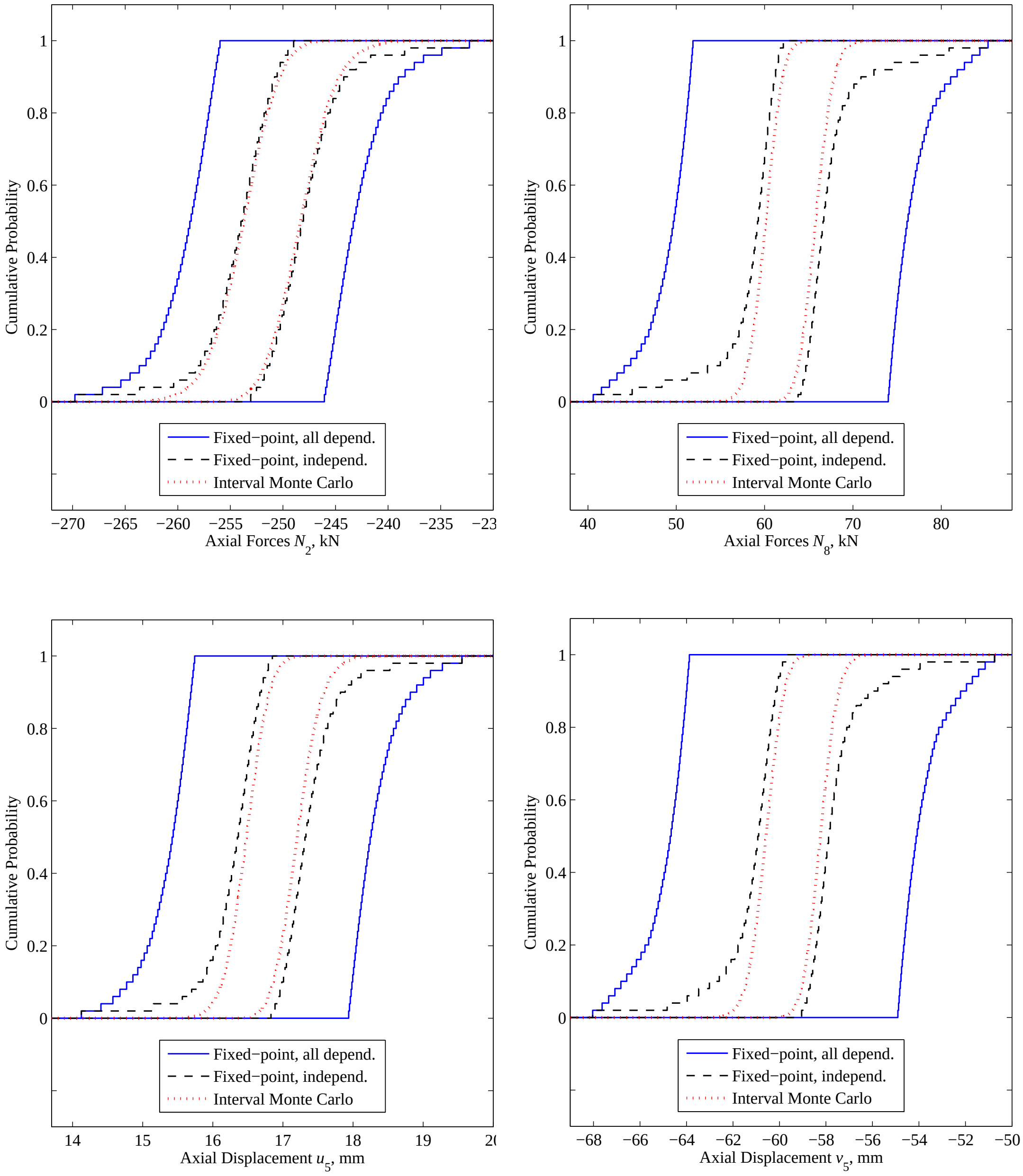


*Figure 4.* P-box solution for the axial force $N_2$ (upper left) and $N_8$ (upper right) and nodal displacements $u_5$ (lower left) and $v_5$ (lower right) of the symmetric simple truss of Figure 3, obtained from: the current method assuming positive dependence for $E_i$ (solid lines), the current method assuming independence (dashed lines), and the interval Monte Carlo method from an ensemble of 100,000 simulations (dotted lines).

depicted in Figure 4. Again, 50 focal elements are used to discretize the p-box. Because there is no simple analytical solution, the current method is compared with the interval Monte Carlo method obtained from 100,000 simulations. For all the results, solution from the current method is wider than the interval Monte Carlo solution and always contains it, even for the deterministic axial force $N_2$. This is not surprising, because the current method considers any dependence between the random variables, while the interval Monte Carlo method can only consider the independent case. Again, the solution obtained from the current method assuming independence between random variables is very close to the interval Monte Carlo solution.

## 5. Conclusion

A new method is presented to solve linear system of equations with p-box entries, together with an application to structural static problems for plane trusses. Uncertainties in the system are modeled as p-boxes, which represent random variables whose CDF lie within the bounds of the p-boxes. The results are also presented in the form of p-boxes. To reduce overestimation in the obtained bounds, a matrix decomposition strategy and a fixed-point formulation are adopted, which are originally used for solving interval linear systems. Numerical examples illustrate that the performance of the current method is satisfactory.

Though the discussion is currently restricted to static analysis trusses, one of the simplest of structure forms, the formulation can be extended to more complicated structures such as frames, plane problems, plates, shells, etc., as well as other types of analysis such as frequency response analysis, vibration analysis, transient analysis, structural damage detection, etc. The introduction of p-boxes in the modeling of uncertainties in these problems will provide useful information about the bounds on the statistical properties of the random variables, regardless of the dependence of the uncertain parameters involved.

## References

Alefeld, G. and J. Herzberger. *Introduction to Interval Computation.* Academic Press, 1984.

Augustin, T. and R. Hable. On the impact of robust statistics on imprecise probability models: A review. *Structural Safety*, 32:358–365, 2010.

Beer, M., S. Ferson and V. Kreinovich. Imprecise probabilities in engineering analyses. *Mechanical Systems and Signal Processing*, 37:4–29, 2013.

Bathe, K. and E. L. Wilson. *Numerical Methods in Finite Element Analysis.* Prentice-Hall, Inc., Englewood Cliffs, New Jersey, 1976.

Clayton, D. G. A model for association in bivariate life tables and its application in epidemiological studies of familial tendency in chronic disease incidence. *Biometrika*, 65(1):141–151, 1978.

Cook, R. D., D. S. Malkus, M. E. Plesha and R. J. Witt. *Concepts and Applications of Finite Element Analysis.* John Wiley & Sons, 2007.

Cui, W. C. and D. I. Blockley. Interval probability theory for evidential support. *International Journal of Intellegent Systems*, 5(2):183–192, 1990.

Davis, J. P. and J. W. Hall. A software-supported process for assembling evidence and handling uncertainty in decision-making. *Decision Support Systems*, 35:414–433, 2003.

Dehghan, M., B. Hashemi and M. Ghatee. Computational methods for solving fully fuzzy linear systems. *Applied Mathematics and Computation*, 179(1):328–343, 2006.

Dempster, A. P. Upper and lower probabilities induced by a muilti-valued mapping. *The Annals of Mathematical Statistics*, 38:325–339, 1967.

Dubois, D. and H. Prade. Random sets and fuzzy interval analysis. *Fuzzy Sets of Systems*, 42:87–101, 1991.

Fernández-Martínez, J. L., Z. Fernández-Muñiz, J. L. G. Pallero and L. M. Pedruelo-González. From Bayes to Tarantola: new insights to understand uncertainty in inverse problems. *Journal of Applied Geophysics*, 98:62–72, 2013.

Ferson, S. *RAMAS Risk Calc 4.0 Software: Risk Assessment with Uncertain Numbers.* Applied Bimathematics, Setauket, New York, 2002.

Ferson, S., L. Ginzburg, V. Kreinovich, L. Longpré and M. Aviles. Exact bounds on finite populations of interval data. *Reliable Computing*, 11(3):207–233, 2005.

Ferson, S., R. B. Nelsen, J. Hajagos, D. J. Berleant, J. Zhang, W. T. Tucker, L. R. Ginzburg and W. L. Oberkampf. Dependence in probabilistic modeling, Dempster-Shafer theory, and probability bounds analysis. *Sandia Report, SAND2004-3072*, 2004.

Frank, M. On the simultaneous associativity of and $F(x, y)$ and $x + y - F(x, y)$. *Aequationes Mathematicae*, 19:194–226, 1979.

Frank, M. J. and B. Schweizer. On the duality of generalized infimal and supremal convolutions. *Rendiconti dí Matematica Series*, 4(12):1–23, 1979.

Fréchet, M. Sur les tableaux de corrélation dont les marges sont données. *Annales de l'Université de Lyon. Section A: Sciences Mathématiques et Astronomie*, 9:53–77, 1951.

Ghanem, R. and P. D. Spanos. *Stochastic Finite Elements: A Spectral Approach.* Springer-Verlag, Berlin, 1991.

Hoeffding, W. Scale-invariant correlation theory. *Collected Works of Wassily Hoeffding*, N. I. Fisher and P. K. Sen (eds.), Springer-Verlag, New York, 1940.

Igusa, T., S. G. Buonopane and B. R. Ellingwood. Bayesian analysis of uncertainty for structural engineering applications. *Structural Safety*, 24(2):165–186, 2002.

Kimeldorf, G. and A. Sampson. Uniform representations of bivariante distributions. *Communications in Statistics*, 4:617–627, 1975.

Klir, G. J. and M. J. Wierman. *Uncertainty-Based Information - Elements of Generalized Information Theory.* Physica-Verlag, Heidelberg, 1999.

Kolmogorov, A. N. *Foundations of the Theory of Probability.* Chelsea Publishing Company, New York, 1950.

Kulisch, U. W. and W. L. Miranker. *Computer Arithmetic in Theory and Practice.* Academic Press, New York, 1981.

Lucas, D. J. Default correlation and credit analysis. *Journal of Fixed Income*, 4(4):76–87, 1995.

Moens, D. and M. Hanss. Non-probabilistic finite element analysis for parametric uncertainty treatment in applied mechanics: Recent advances. *Finite Elements in Analysis and Design*, 47(1):4–16, 2011.

Moore, R. E., R. B. Kearfott and M. J. Cloud. *Introduction to Interval Analysis.* Society for Industrial and Applied Mathematics, 2009.

Muhanna, R. L. and R. L. Mullen. Uncertainty in mechanics problems – interval-based approach. *Journal of Engineering Mechanics*, American Society of Civil Engineers, 127(6):557–566, 2001.

Muhanna, R. L., H. Zhang and R. L. Mullen. Combined axial and bending stiffness in interval finite-element methods. *Journal of Structural Engineering*, 133(12):1700–1709, 2007.

Nelsen, R. B. *An Introduction to Copulas.* Lecture Notes in Statistics 139, Springer-Verlag, New York, 1999.

Neumaier, A. and A. Pownuk. Linear systems with large uncertainties, with applications to truss structures. *Reliable Computing*, 13(2):149–172, 2007.

Rama Rao, M. V., R. L. Mullen and R. L. Muhanna. A new interval finite element formulation with the same accuracy in primary and derived variables. *International Journal of Reliability and Safety*, 5(3/4):336–367, 2011.

Shafer, G. *A Mathematical Theory of Evidence.* Princeton University Press, Princeton, 1968.

Sklar, A. Fonctions de répartition à $n$ dimensions et leurs marges. *Publications de L'Institut de Statistiques de l'Université de Paris*, 8:229–231, 1959.

Soize, C. Bayesian posteriors of uncertainty quantification in computational structural dynamics for low-and medium-frequency ranges. *Computers & Structures*, 126:41–55, 2013.

Williamson, R. C. *Probabilistic Arithmetic*. University of Queensland, PhD Thesis, 1989.

Xiao, N. *Interval Finite Element Approach for Inverse Problem under Uncertainty.* Georgia Institute of Technology, PhD Thesis, 2015.

Xiao, N., R. L. Muhanna, F. Fedele and R. L. Mullen. Uncertainty analysis of static plane problems by intervals. *SAE International Journal of Materials and Manufacturing*, 8:374–381, 2015.

Zhang, H. *Nondeterministic Linear Static Finite Element Analysis: an Interval Approach.* Georgia Institute of Technology, PhD Thesis, 2005.

Zhang, J. and B. Ellingwood. Orthogonal series expansions of random fields in reliability analysis. *Journal of Engineering Mechanics (ASCE)*, 120:2660–2677, 1994.

Zhang, H., R. L. Mullen and R. L. Muhanna. Structural analysis with probability-boxes. *International Journal of Reliability and Safety*, 6(1/2/3):110–129, 2012.